ICES Journal of Marine Science

ICES Journal of Marine Science (2018), doi:10.1093/icesjms/fsy074

Contribution to the Themed Issue: '*Mesopelagic resources*'

Trophic ecology of meso- and bathypelagic predatory fishes in the Gulf of Mexico

Travis M. Richards[1,*], Emily E. Gipson[2], April Cook[3], Tracey T. Sutton[3], and R. J. David Wells[1,4]

[1]*Department of Marine Biology, Texas A&M University at Galveston, 1001 Texas Clipper Rd., Galveston, TX 77553, USA*
[2]*Department of Biology, University of Central Florida, Orlando, FL 32816, USA*
[3]*Halmos College of Natural Sciences and Oceanography, Nova Southeastern University, Dania Beach, FL, USA*
[4]*Department of Wildlife and Fisheries Sciences, Texas A&M University, College Station, TX 77843, USA*

**Corresponding author: tel: +1 409 740 4529; fax: +1 409 740 5001; e-mail: travis.richards3@gmail.com.*

Richards, T. M., Gipson, E. E., Cook, A., Sutton, T. T., and Wells, R. J. D. Trophic ecology of meso- and bathypelagic predatory fishes in the Gulf of Mexico. – ICES Journal of Marine Science, doi:10.1093/icesjms/fsy074.

Received 15 January 2018; revised 29 May 2018; accepted 30 May 2018

The trophic ecology of eight circumglobal meso- and bathypelagic fishes (*Anoplogaster cornuta*, *Chauliodus sloani*, *Coccorella atlantica*, *Gigantura chuni*, *G. indica*, *Omosudis lowii*, *Photostomias guernei*, and *Stomias affinis*) with contrasting vertical migration habits (vertical migrators vs. non-migrators) were examined using stable isotope analysis (SIA). Mean $\delta^{13}C$ values of these predators were similar among species, ranging from −18.17 to −18.99 ‰, suggesting that all species are supported by a similar carbon source. This finding was supported by mixing-model analysis; all of these deep-living predators received the majority (>73%) of their carbon from epipelagic food resources. Mean $\delta^{15}N$ values of the predators ranged from 9.18 to 11.13 ‰, resulting in trophic position estimates between the third and fourth trophic level, although significant shifts in $\delta^{15}N$ with increasing body size suggest that some of these species undergo ontogenetic shifts in trophic position. Bayesian standard ellipses, used to estimate isotopic niche areas, differed in size among species, with those occupying the highest relative trophic positions possessing the largest isotopic niches. These results, which provide the first trophic descriptions using dietary tracers for several of these species, offer insight into the trophic structure of deep-sea ecosystems and will help inform the construction of ecosystem-based models.

Keywords: bathypelagic, epipelagic, feeding ecology, mesopelagic, mixing models, stable isotopes

Introduction

The deep-pelagic zone (waters deeper than 200 m to just above the seabed) represents the largest cumulative habitat on earth and is home to a diverse array of specialized fauna adapted to its abiotic and biotic conditions (Angel, 1997; Robison, 2004, 2009). The deep sea and its inhabitants provide an array of ecosystem services that are important to humans, including carbon sequestration, nutrient regeneration, fisheries production, and waste absorption (Danovaro *et al.*, 2008; Mengerink *et al.*, 2014; Thurber *et al.*, 2014). Despite its enormous volume and the economic and ecological importance of its fauna, deep-pelagic ecosystems remain chronically understudied (Webb *et al.*, 2010) and face an increasing number of stressors including climate change, ocean acidification, overfishing, and natural resource extraction (Morato *et al.*, 2006; Ramirez-Llodra *et al.*, 2011; Mengerink *et al.*, 2014). As threats to the diversity and stability of marine ecosystems increase and expand into deeper oceanic environments, there has been increasing concern regarding the status of deep-sea communities and a renewed interest in describing and understanding deep-sea ecosystem structure.

Central to our understanding of ecosystem and community structure is a thorough knowledge of foodwebs (Polis and Strong, 1996; McCann, 2000). In addition to providing important information regarding ecosystem functioning, the study of foodwebs provides understanding of how animal communities are structured and sheds light on the mechanisms underlying species coexistence and persistence. While our knowledge of deep-pelagic foodwebs has advanced considerably over the past few decades

(Robison, 2009; Sutton, 2013), fundamental information in many regions, including species-specific feeding relationships, trophic position estimates, and delineations of energy pathways connecting disparate trophic levels and communities, is lacking (Mengerink *et al.*, 2014; Drazen and Sutton, 2017).

Fishes are a dominant component of deep-pelagic ecosystems worldwide and are among the main taxa that undertake diel vertical migrations (DVM). While the standardized abundance (no. per unit volume) of meso- and bathypelagic fishes is relatively low (Angel and Baker, 1982), their global distributions have resulted in high cumulative biomass estimated at 7–10 billion tonnes (Gjøsaeter and Kawaguchi, 1980; Irigoien *et al.*, 2014). Due to their sheer numbers and vertical migration behaviour, which can exceed 1000 m in vertical extent, it is increasingly being recognized that fishes play key ecological and biogeochemical roles in open-ocean ecosystems (Wilson *et al.*, 2009; Drazen and Sutton, 2017). As highly abundant mid-level consumers, deep-pelagic fishes help regulate zooplankton populations (Hopkins and Gartner, 1992; Pakhomov *et al.*, 1996). Deep-pelagic fishes also serve as trophic links between zooplankton and higher-order consumers such as epipelagic fishes (Moteki *et al.*, 2001; Choy *et al.*, 2013), marine mammals (Pauly *et al.*, 1998), and seabirds (Raclot *et al.*, 1998; Cherel *et al.*, 2008). DVM of fishes have been shown to connect the epi-, meso-, and bathypelagic habitats with each other and with deep-benthic habitats (Porteiro and Sutton, 2007; Trueman *et al.*, 2014).

Stable isotope analysis (SIA) has been widely used to delineate foodweb structure and provides an integrated view of an organism's diet over time-scales relevant to tissue turnover rates rather than digestion rates (Peterson and Fry, 1987; Post, 2002). Carbon isotopes undergo relatively small amounts of fractionation during trophic transfers and are useful for determining the relative contributions of carbon sources to the production of consumers (Peterson and Fry, 1987). Stable isotopes of nitrogen undergo comparatively large levels of fractionation (~3–5 ‰) during trophic transfer, resulting in predictable differences in the isotopic signatures of consumers and their prey (Post, 2002; Hussey *et al.*, 2014). The relatively predictable level of enrichment of ^{15}N during trophic transfer allows for the determination of trophic levels and can be used to identify trophic relationships within assemblages of organisms (Peterson and Fry, 1987; Post, 2002).

To date, much of the research describing the trophic ecology of deep-pelagic fishes has focused on zooplanktivorous groups (myctophids, sternoptychids, gonostomatids), while less attention has been paid to micronektonivores (stomiids, alepisauroids) that occupy higher trophic levels. The numerical importance of micronektonivores (Hopkins *et al.*, 1996; Sutton and Hopkins, 1996a), their propensity to prey heavily on zooplanktivorous fishes (Clarke, 1982; Hopkins *et al.*, 1996; Sutton and Hopkins, 1996b), and documented importance as prey for higher trophic level consumers (Moteki *et al.*, 2001; Choy *et al.*, 2013) provides the rationale for further describing their trophic dynamics. Here, we describe the trophic ecology of eight putative high-trophic-level fishes: *Anoplogaster cornuta*, *Chauliodus sloani*, *Coccorella atlantica*, *Gigantra chuni*, *G. indica*, *Omosudis lowii*, *Photostomias guernei*, and *Stomias affinis*. These species are meso- and bathypelagic fishes with circumglobal distributions, some of which have been documented as numerically important components of deep-pelagic assemblages (Sutton and Hopkins, 1996a; Moore *et al.*, 2003; Sutton *et al.*, 2008). Specific goals of this study are to provide estimates of trophic position, describe the isotopic niche areas and the extent of niche overlap among species, detail ontogenetic shifts in trophic position, and quantify the relative carbon contributions of particulate organic matter (POM) from the epi-, meso-, and bathypelagic zones to each of these species.

Material and methods

Sample collection and study site

Fishes were collected from the northern Gulf of Mexico (GOM) during three oceanographic cruises conducted during 2011 in spring (22 March–11 April), summer (23 June–13 July), and fall (8–27 September). All cruises were part of the Offshore Nekton Sampling and Analysis Program (ONSAP) that was implemented following the *Deepwater Horizon* oil spill in support of NOAA's Natural Resource Damage Assessment (NRDA). ONSAP stations are the same as stations currently used by the long-term Southeast Area Monitoring and Assessment Program (SEAMAP) and are situated every half degree of longitude and latitude in the northern GOM (Figure 1). Specimens were collected using large midwater trawls fitted with large-mesh panels (~80 cm) near the mouth that gradually tapered to smaller mesh (~6 cm) sizes before the codend. Trawls were fished obliquely from the surface to depths of either 700 or 1400 m. Once the trawls were retrieved, animals were sorted, enumerated, and visually identified to species. Samples for SIA were selected haphazardly in an effort to maximize spatial and temporal coverage. All specimens for SIA were frozen whole at –20°C until processed at Texas A&M University at Galveston.

Stable isotope analysis

SIA was conducted on 212 specimens, with sample sizes of each species ranging from 19 to 37 individuals (Table 1). White muscle tissue for SIA was dissected from the dorsal musculature of fishes and visually examined under a dissecting microscope for the presence of bones, which were subsequently removed. Cleaned samples were rinsed with deionized water, frozen, and lyophilized for 48 h. Freeze-dried samples were homogenized using a mortar and pestle, weighed, wrapped in tin capsules, and shipped to the Stable Isotope Facility at the University of California Davis for analysis. Analysis of muscle tissue δ^{13}C and δ^{15}N was carried out using an elemental analyser (PDZ Europa ANCA-GSL) coupled with an isotope ratio mass spectrometer (PDZ Europa 20-20). The long-term standard deviation of the facility at UC Davis is 0.2 ‰ for δ^{13}C and 0.3 ‰ for δ^{15}N. Stable isotope data are expressed relative to international standards of Vienna PeeDee belemnite and atmospheric N_2 for carbon and nitrogen, respectively. The C: N of fishes in this study were low (species mean C: N range 3.31–3.86; 92% of individuals C: N < 4.0) compared with C: N from similar species collected in the Atlantic and Southern oceans (C: N 3.3–12.5; Hoffman and Sutton, 2010), suggesting that lipids did not significantly confound the interpretation of δ^{13}C data. Therefore, all statistical analyses were performed on uncorrected δ^{13}C values.

The stable isotope data of POM used in this study are derived from the published dataset of Fernández-Carrera *et al.* (2016). For detailed descriptions of methodologies and sample locations, see Fernández-Carrera et al. (2016), but a brief description of methodologies follows. POM samples were collected during summer 2011 (2–21 July) in the northern GOM. In addition to samples collected in pelagic waters, the complete published dataset included samples taken from waters over the continental shelf

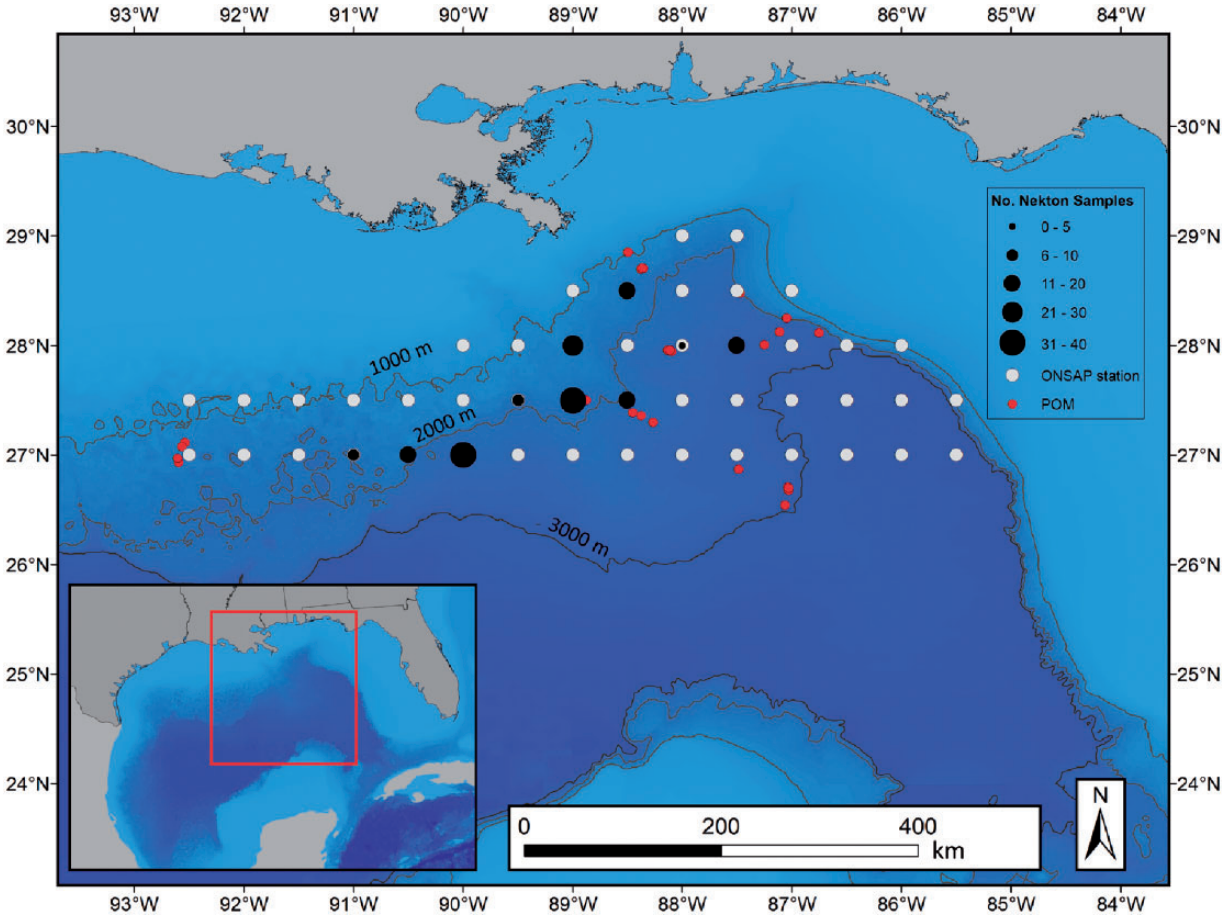

Figure 1. Map of ONSAP sampling grid, locations of POM samples, and locations where fishes were collected for SIA (specimen number denoted by circle diameter) in the GOM.

Table 1. Species-specific sample descriptions and bulk $\delta^{13}C$ and $\delta^{15}N$ isotope data (mean ± *SD*).

Species	*n*	Spring	Summer	Fall	Standard length range (mm)	Mean standard length (mm) ± *SD*	$\delta^{13}C$ (‰) ± *SD*	$\delta^{15}N$ (‰) ± *SD*	C: N_{bulk} ± *SD*
A. cornuta[1]	23	2	12	9	84–148	114.35 ± 19.09	−18.93 ± 0.67	11.14 ± 0.96	3.66 ± 0.44
C. sloani[2]	30	10	20	0	143–237	191.43 ± 23.32	−18.68 ± 0.43	9.51 ± 0.42	3.42 ± 0.23
C. atlantica[2]	19	0	19	0	44–125	89.53 ± 26.53	−18.50 ± 0.47	9.96 ± 0.83	3.67 ± 0.34
G. chuni[1]	24	6	9	9	34–186	134.57 ± 40.11	−18.25 ± 0.44	11.13 ± 1.08	3.31 ± 0.15
G. indica[1]	21	8	6	7	75–192	141.95 ± 28.83	−18.25 ± 0.94	10.70 ± 0.64	3.43 ± 0.29
O. lowii[1]	32	12	10	10	36–261	120.66 ± 61.60	−19.04 ± 0.32	9.79 ± 0.60	3.40 ± 0.08
P. guernei[2]	37	14	13	10	56–127	98.08 ± 14.03	−18.61 ± 0.40	9.18 ± 0.63	3.44 ± 0.13
S. affinis[2]	26	5	16	5	55–205	127.31 ± 38.66	−19.38 ± 0.84	9.98 ± 0.89	3.86 ± 0.63

[1]Denotes no DVM, [2]denotes asynchronous DVM (not all individuals of population migrate vertically each day). References for vertical migration patterns: *A. cornuta* (Clarke and Wagner, 1976), *C. sloani* (Sutton and Hopkins, 1996a), *C. atlantica* (McEachran and Fechhelm, 1998), *G. chuni* (McEachran and Fechhelm, 1998), *G. indica* (Sutton *et al.*, 2010), *O. lowii* (McEachran and Fechhelm, 1998; Sutton *et al.*, 2010), *P. guernei* (Sutton and Hopkins, 1996a), *S. affinis* (Sutton and Hopkins, 1996a).

and from waters in close proximity to the Mississippi River. In order to maximize the spatial overlap between POM samples and the collection locations of fishes, only POM data collected within close proximity to ONSAP sampling stations in waters ≥1000 m deep (Figure 1) were utilized. POM samples were collected throughout the water column using remotely fired 10-l Niskin bottles. Samples were then filtered across 47-mm glass fibre filters at low pressure and dried at 60°C for 24 h prior to isotope analysis (Fernández-Carrera et al., 2016). In order to determine if the isotopic signatures of POM samples changed with depth, we used collection depth to designate POM samples as epipelagic (0–200 m), mesopelagic (200–1000 m), or bathypelagic (>1000 m) so that statistical comparisons could be made.

Data analysis

Multivariate analysis of variance (MANOVA) was used to test for differences in $\delta^{13}C$ and $\delta^{15}N$ among species and POM depth

zones. Species and season were included as factors in the linear model and tested for the presence of an interaction. If significant differences were found, univariate tests for both $\delta^{13}C$ and $\delta^{15}N$ were performed using analysis of variance among fish species and POM depth zones. *A posteriori* differences among means were detected using Tukey's honestly significant difference (HSD) test. Using equation 4 from Post *et al.* (2007), trophic position was calculated for each species:

$$TrL_i = [(\delta^{15}N_i - \delta^{15}N_{base})/\Delta^{15}N] + \lambda \quad (1)$$

where $\delta^{15}N_i$ is the mean species $\delta^{15}N$, $\delta^{15}N_{base}$ is the mean $\delta^{15}N$ of the primary producer or primary consumer being used to set the isotopic baseline, $\Delta^{15}N$ is the trophic discrimination factor, and λ represents the trophic level of the organism being used to set the baseline. Because primary consumer data were not available for the time-period of this study, trophic position estimates made using mean $\delta^{15}N$ values of POM collected from the epipelagic zone were compared with estimates calculated from published $\delta^{15}N$ values of a group of primary consumers (euphausiids) collected in the pelagic northern GOM during 2007 (McClain-Counts *et al.*, 2017). In order to explore the relationship between fish size and $\delta^{13}C$ and $\delta^{15}N$, least-squares linear regression analysis was conducted for each species. Spatial variation in $\delta^{13}C$ and $\delta^{15}N$ of both fishes and POM was investigated using least-squares linear regression between isotopic values and longitude and latitude (0.5° intervals). Because every species was not collected at every sampling location, isotope data were pooled across species within each line of longitude and latitude (more than one site along each 0.5° of longitude). Additionally, because not all species were collected across a range of latitudes and longitudes within each season, the effect of season on the spatial relationships of the isotope data was not explored. All statistical analyses were performed in R (R Development Core Team, 2016) v. 3.3.2.

The trophic breadth of each species and trophic similarity among species were assessed by calculating standard ellipse areas (SEA) using the R package SIBER (Jackson *et al.*, 2011) and following methods outlined by Jackson *et al.* (2011). Bayesian standard ellipses encompass ~40% of the isotope data for each species are less affected by increases in sample size or statistical outliers than convex hull analysis, and represent the core isotopic niche area of a species (Jackson *et al.*, 2011). Size-corrected SEAs (SEA_c) were calculated for each species, which adjusts for underestimation of ellipse area at small sample sizes and allows for comparison of ellipse sizes to other studies (Jackson *et al.*, 2011). Overlap of size-corrected ellipses was used as a proxy for trophic similarity and was examined by calculating the extent of overlap between each pairwise combination of species. The percentage of overlap between species pairs was calculated by dividing the area of overlap ($‰^2$) by the total combined ellipse area ($‰^2$) of the two species being compared. Isotopic niche overlap was considered significant when overlap between two species was >50%. Differences in size-corrected ellipse area, a proxy for trophic breadth that assumes species with larger SEAc feed more broadly within the foodweb than those with smaller SEAc were compared among species and considered to be significantly different when 95% of posterior draws were smaller in one species compared with the other.

The Bayesian mixing model, MixSIAR (Stock and Semmens, 2015), was used to estimate the relative contribution of epi- (0–200 m), meso- (200–1000 m), and bathypelagic (>1000 m) POM to each species. Bayesian mixing models provide the most accurate estimations of source or prey contributions when tissue and species-specific discrimination factors are used (Caut *et al.*, 2008), but discrimination factors for meso- and bathypelagic fishes are currently unknown. We chose to run mixing models using discrimination factors of 3.15 ‰ ± 1.28 ‰ and 0.97 ‰ ± 1.08 ‰ for $\delta^{15}N$ and $\delta^{13}C$, respectively (Sweeting *et al.*, 2007a,b), which have been previously used to study the trophic structure of meso- and bathypelagic fishes (Valls *et al.*, 2014). Mixing models in MixSIAR estimate probability density functions using Markov chain Monte Carlo methods, and each model was run with identical parameters (number of chains = 3; chain length = 100 000; burn in = 50 000; thin = 50). Model convergence was determined using Gelman-Rubin and Geweke diagnostic tests (Stock and Semmens, 2015).

Results

Stable isotopes

Individual consumer $\delta^{13}C$ values ranged from –21.49 to –16.63 ‰, while mean $\delta^{13}C$ values were similar among species, with a difference of 1.13 ‰ separating the most depleted (*S. affinis*: –19.38 ‰ ± 0.83) and most enriched species (*G. chuni*: –18.25 ‰ ± 0.44 and *G. indica*: –18.25 ‰ ± 0.94) (Table 1; Figure 2). Individual $\delta^{15}N$ values varied between 7.10 and 13.07 ‰, with 1.96 ‰ separating the mean $\delta^{15}N$ values of the most enriched (*A. cornuta*: 11.14 ‰ ± 0.96) and depleted species (*P. guernei*: 9.18 ‰ ± 0.63) (Table 1; Figure 2). Species-specific differences in $\delta^{13}C$ and $\delta^{15}N$ were significant ($F_{14,\ 382} = 17.24$, $p < 0.001$); however, no significant seasonal effects were found ($F_{14\ 382} = 1.29$, $p = 0.27$), and no significant interaction effect among species and season was detected ($F_{22\ 382} = 1.05$, $p = 0.40$). Significant differences in $\delta^{13}C$ values among species (one-way ANOVA; $F_{7204} = 11.62$, $p < 0.001$) were driven by *G. chuni* and *G. indica*, which were enriched in ^{13}C compared with more ^{13}C-depleted species such as *O. lowii* and *S. affinis* (Figure 2). Significant differences in $\delta^{15}N$ among species (one-way ANOVA; $F_{7204} = 25.55$, $p < 0.001$) were primarily driven by *A. cornuta*, *G. chuni*, and *G. indica*, which were enriched in ^{15}N compared with *C. sloani* and *P. guernei* (Figure 2). Results of all pairwise comparisons for $\delta^{13}C$ and $\delta^{15}N$ values among species are listed in Supplementary Table S1.

The $\delta^{13}C$ values of fishes were significantly correlated with latitude ($r = 0.08$, $p < 0.01$) and longitude ($r = 0.04$, $p < 0.01$), while $\delta^{15}N$ values were not (latitude $p = 0.46$; longitude $p = 0.19$). Due to limited spatial coverage within each species, spatial trends were tested by pooling all fish species together. Because spatial variation could not be tested within each species and due to the low correlation coefficients observed among fish $\delta^{13}C$ values and latitude and longitude, isotope data for each species were pooled across lines of latitude and longitude during subsequent analysis.

A total of 154 samples of POM collected from depths ranging from 1 to 2500 m were utilized (Fernández-Carrera et al. 2016). POM exhibited a wide range of $\delta^{13}C$ (–27.17 to –16.41) and $\delta^{15}N$ values (–3.58 to 11.69), with POM samples generally becoming more ^{15}N enriched with increasing depth (Figure 2). Significant differences in POM $\delta^{13}C$ and $\delta^{15}N$ among vertical depth zones (MANOVA: $F_{4302} = 14.54$, $p < 0.001$) were observed. Significant differences in $\delta^{15}N$ were found among depth zones (ANOVA:

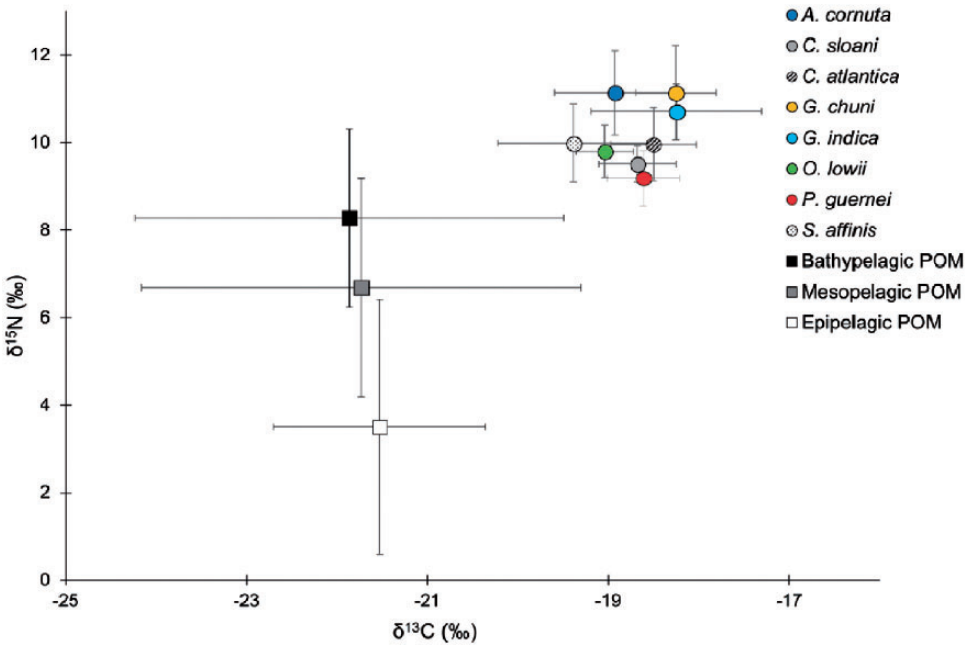

Figure 2. Isotope bi-plot of $\delta^{13}C$ and $\delta^{15}N$ values from POM (squares) and fishes (circles). Data points represent means and error bars represent ± 1 *SD*.

$F_{2151} = 34.41$, $p < 0.001$), with epipelagic POM more ^{15}N depleted than POM collected from mesopelagic and bathypelagic depths ($p < 0.001$). The $\delta^{13}C$ values of POM did not significantly differ across depth zones ($F_{2151} = 0.42$, $p = 0.66$). Latitudinal and longitudinal variation in POM $\delta^{13}C$ and $\delta^{15}N$ was minimal, with the only significant correlation occurring between epipelagic POM $\delta^{13}C$ and longitude, although correlation coefficients were low ($r = 0.04$, $p = 0.043$). All other pairwise combinations between $\delta^{13}C$ and $\delta^{15}N$ and latitude or longitude within the epi-, meso-, and bathypelagic depth zones were non-significant (Supplementary Table S2).

Trophic position estimates

The use of primary producers or primary consumers to set the isotopic baseline had no effect on the relative trophic positions among consumers, but resulted in slight differences (0.32 TL) in calculated trophic levels. When primary producer (POM) data were used to set the baseline, consumer TPs ranged from 2.8 (*P. guernei*) to 3.4 (*A. cornuta, G. chuni*), while all species fell within the third and fourth trophic levels when primary consumers were used to set the baseline (*P. guernei* = 3.1, *A. cornuta* and *G. chuni* = 3.7) (Figure 3; Supplementary Table S3).

Of the species examined, *A. cornuta* ($r = 0.63$, $p < 0.001$), *C. atlantica* ($r = 0.74$, $p < 0.001$), *G. chuni* ($r = 0.41$, $p < 0.001$), *C. sloani* ($r = 0.22$, $p < 0.001$), *P. guernei* ($r = 0.25$, $p < 0.001$), and *S. affinis* ($r = 0.53$, $p < 0.001$) exhibited significant positive relationships between $\delta^{15}N$ and SL (Figure 4). Relationships between $\delta^{13}C$ and SL were more variable than those observed with $\delta^{15}N$ (Figure 4). Two species, *G. chuni* ($r = 0.33$, $p < 0.01$) and *O. lowii* ($r = 0.44$, $p < 0.001$) displayed significant positive relationships between $\delta^{13}C$ and SL (Figure 4).

Isotopic niche breadth, calculated using SEA_c, was largest for the piscivorous *S. affinis* ($SEA_c = 2.27$), *G. indica* ($SEA_c = 1.98$), *A. cornuta* ($SEA_c = 1.96$), and *G. chuni* ($SEA_c = 1.53$), which collectively occupied the highest trophic positions within the guild of predators examined. *C. atlantica* ($SEA_c = 0.1.19$) occupied an intermediate relative trophic position and intermediate-sized trophic niche. *P. guernei* ($SEA_c = 0.71$) and *O. lowii* ($SEA_c = 0.62$), which feed primarily on crustaceans and cephalopods, respectively, occupied lower relative trophic positions and were characterized by relatively small isotopic niches (Figure 5, Table 2). Interestingly, the smallest isotopic niche also belonged to a known piscivore, *C. sloani* ($SEA_c = 0.56$), although the small calculated isotopic niche area could have been due to a limited sampled size range (Figure 4). In the 20 instances where overlap in SEAc occurred, the percentage of shared isotopic niche space ranged from 1% (*A. cornuta* and *C. atlantica; G. indica and O. lowii*) to 27% (between *G. chuni* and *G. indica*) (Table 3). Directional overlap, or the percentage of one species' ellipse covering the ellipse of another species, varied widely from 2 to 100%. Differences in directional overlap was greatest between *C. sloani* and *C. atlantica* (81 vs. 38%), *C. sloani* and *S. affinis* (63 vs. 15%), and *O. lowii* and *S. affinis* (100 vs. 27%) (Table 3, Figure 5).

Mean POM $\delta^{13}C$ and $\delta^{15}N$ values collected from the meso- and bathypelagic were not significantly different from each other, thus mixing models were run using epipelagic POM data and data combined from the meso- and bathypelagic zones. Mixing model results suggest that all consumers included in this study derive the bulk of their carbon from epipelagic POM (Figure 6). Relative contributions of epipelagic POM ranged from 97.87% ± 1.43 in *P. guernei* to 73.30% ± 3.19 in *G. chuni*, while contributions from meso- and bathypelagic POM were much lower, ranging from 26.70% ± 3.19 in *G. chuni* to 2.13% ± 1.43 in *P. guernei*. Diagnostic plots of posterior distributions revealed a high negative correlation between the two sources (epipelagic POM and meso-/bathypelagic POM). Considering that the producer data fully constrain consumer data when an appropriate trophic enrichment factor is applied and that model diagnostics (Gelman-Rubin Diagnostic: all variables <1.01; Gweke

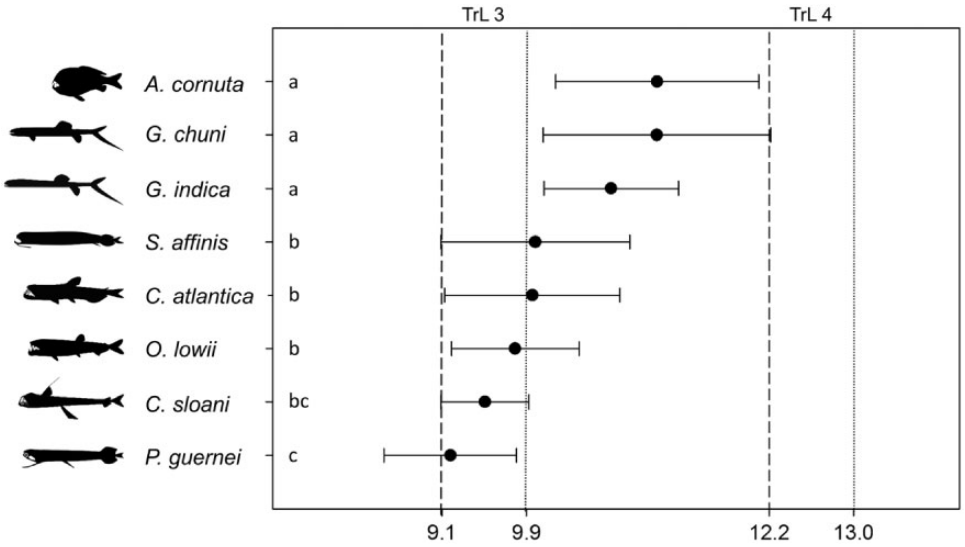

Figure 3. Trophic level estimates calculated using δ^{15}N data of each species. Letters represent significant differences in TL among species, with like letters being similar and non-like letters significantly different. Dashed lines represent the δ^{15}N threshold values of TL 3 and TL 4 when using primary consumers (euphausiids) to set the isotopic baseline; dotted lines represent the δ^{15}N threshold values of TL 3 and TL 4 when using primary producers (POM) to establish isotopic baseline. For species-specific TP estimates ($\pm$ *SD*), see Supplementary Table S3.

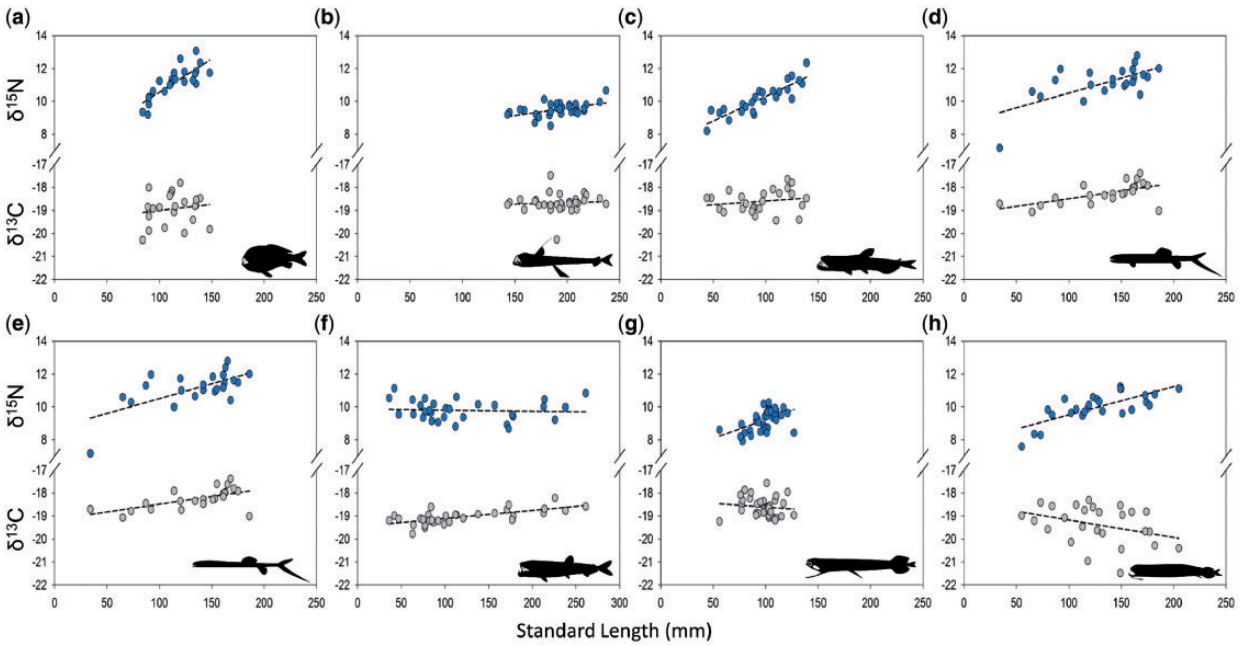

Figure 4. Results of least-squares regression analysis between standard length (mm) and δ^{15}N and δ^{13}C values: (a) *A. cornuta*, (b) *C. sloani*, (c) *C. atlantica*, (d) *G. chuni*, (e) *G. indica*, (f) *O. lowii*, (g) *P. guernei*, and (h) *S. affinis*.

Diagnostic: <5% of variables outside $\pm$1.96 for each chain) indicate that the model fully converged, the negative correlation is likely caused by the similar δ^{13}C signatures of sources and not from a missing carbon source.

Discussion

Trophic structure

Trophic positions inferred through stable isotope data suggest that, within this group of fishes, the highest trophic positions are held by the largely piscivorous *A. cornuta*, *G. chuni*, *G. indica*, and *S. affinis*; intermediate trophic positions are occupied by species preying on mixtures of cephalopods and fishes (*C. atlantica* and *O. lowii*), and fishes and crustaceans (*C. sloani*); and the lowest trophic position is occupied by *P. guernei*, which eats primarily macrocrustaceans (Hopkins *et al.*, 1996; Sutton and Hopkins, 1996b). Stomach content analysis (SCA) was performed on all samples in this study, and though sample sizes with identifiable food items were relatively small, results agree with findings from previous SCA studies and support the trophic relationships inferred through SIA (Supplementary Table S4).

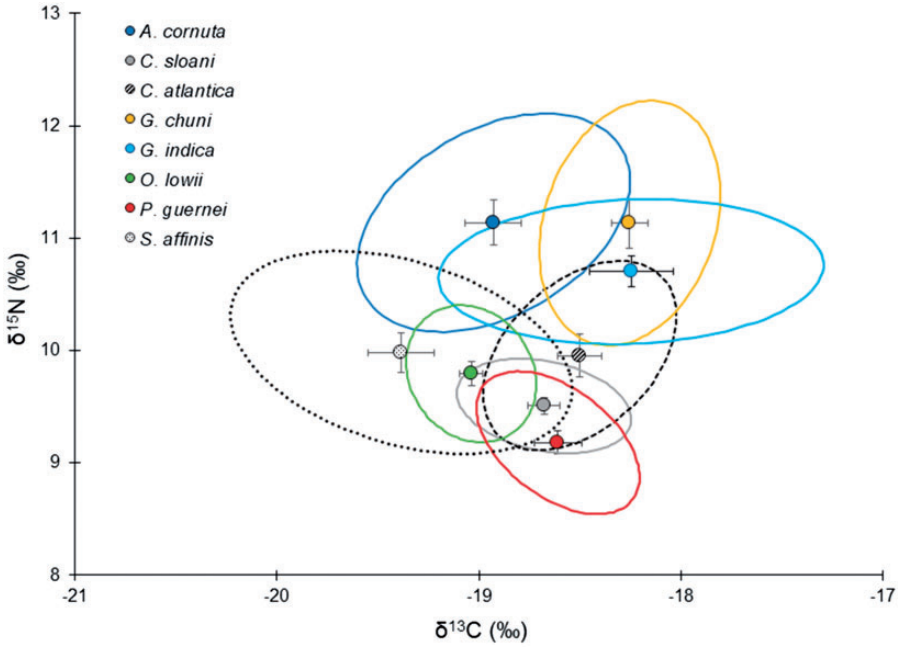

Figure 5. Size-corrected SEAc plotted with mean (± s.e.) $\delta^{13}C$ and $\delta^{15}N$ values for each species.

Table 2. Metrics for estimating isotopic niche size in eight meso- and bathypelagic predators.

Species	TA	SEA	SEAc	CD
A. cornuta	6.81	1.87	1.96	0.97
C. sloani	2.68	0.53	0.56	0.46
C. atlantica	3.02	1.13	1.19	0.82
G. chuni	5.82	1.46	1.53	0.83
G. indica	5.17	1.88	1.98	0.98
O. lowii	2.33	0.60	0.62	0.58
P. guernei	2.58	0.69	0.71	0.66
S. affinis	7.01	2.18	2.27	1.04

TA, total area (expressed in ‰) encompassed by all data points of each species; SEA, standardized ellipse area for each species; SEAc, size-corrected standardized ellipse area; CD, centroid distance calculated by taking average distance of each data point from the centroid for each species.

For the species examined, $\delta^{15}N$ values spanned 5.91 ‰ or 1.9 TLs, while species mean $\delta^{15}N$ values spanned 1.96 ‰ and 0.62 TL (assuming TEF of 3.15). Using mean $\delta^{15}N$ values and applying a TEF of 3.15, our observed range of estimated trophic levels (0.62) appears to be in line with other studies examining Mediterranean (1.1 TLs), Pacific (1.6 TLs), and GOM (1.1 TLs) fish assemblages that included both micronektonivores (stomiids, anoplogastrids) and lower trophic level zooplanktivores (myctophids, gonostomatids), which have been shown to be up to 0.6 TLs lower than micronektonivores (Valls *et al.*, 2014; Choy *et al.*, 2015; McClain-Counts *et al.*, 2017).

Trophic level estimates determined using a primary consumer to set the isotopic baseline placed each species between the third and fourth trophic levels. Where species-specific comparisons of trophic positions could be made, and applying a $\delta^{15}N$ TEF of 3.15 to reported mean $\delta^{15}N$ values, our estimated TPs for *A. cornuta* (3.7) and *C. sloani* (3.2) were similar to estimates from the Pacific (TP = 3.5 for both species) and to the GOM (*C. sloani* TP = 2.8) (Choy *et al.*, 2015; McClain-Counts *et al.*, 2017). The observed difference in TP estimates for *C. sloani* in the GOM was likely caused by the inclusion of smaller *C. sloani* (<50 mm SL) by McClain-Counts *et al.* (2017). Estimates of TP for *S. affinis* (3.4) were similar to *Stomias boa* collected in the Mediterranean (TP = 3.5) (Valls *et al.*, 2014), while estimates of the three stomiid species [*C. sloani* (3.2), *S. affinis* (3.4), and *P. guernei* (3.1)] were within the estimated worldwide TP range of stomiid fishes (TP = 3.0–3.5) (Choy *et al.*, 2012). This study represents the first descriptions of trophic positions using SIA for *C. atlantica*, *G. chuni*, *G. indica*, *O. lowii*, and *P. guernei*, so comparisons to TP estimates in other studies were not possible.

Isotopic niche size, estimated using SEAc, was largest for fishes occupying the highest TPs within the guild (*A. cornuta*, *C. chuni*, *G. indica*, *S. affinis*) and smallest in fishes occupying intermediate and lower TPs (Figure 5). The larger SEAc of the highest TP fishes within this guild could suggest more generalized feeding compared with other species. Differences in SEAc can also be influenced by an organism's size distribution, which was not equally comprehensive in all species. The small SEAc of *C. sloani*, for example, was likely affected by samples that only included the largest individuals (>140 mm SL). Isotopic niche overlap was common, although the extent of the overlap was typically non-significant (<50%) (Table 3). In species where isotopic niche overlap was significant (*S. affinis* and *O. lowii*), available SCA data suggest prey resource overlap is not as strong as isotopic niche overlap would make them appear (Hopkins *et al.*, 1996; Sutton and Hopkins, 1996b).

Samples of POM were more ^{13}C depleted at eastern longitudes that are closer in proximity to the Mississippi River, while fishes became more ^{13}C enriched at southern latitudes and western longitudes. Shifts in the isotopic signatures of POM in the GOM have been observed between nearshore and offshore regions and

Table 3. Isotopic niche overlap measured in percentage of shared space (‰) between each pairwise combination of species.

	A. cornuta		*C. sloani*		*C. atlantica*		*G. chuni*		*G. indica*		*O. lowii*		*P. guernei*	
C. sloani	0 (0, 0)	**0**												
C. atlantica	1 (2, 3)	**0.05**	26 (**81**, 38)	**0.99**										
G. chuni	9 (23, 30)	0.19	0 (0, 0)	**0.99**	14 (32, 25)	0.80								
G. indica	16 (33, 32)	0.49	0 (0, 0)	**0.99**	20 (41, 25)	0.94	27 (**61**, 47)	0.80						
O. lowii	3 (4, 12)	**0**	18 (39, 34)	0.66	11 (16, 32)	**0.01**	0 (0, 0)	**0.01**	1 (2, 5)	**0**				
P. guernei	0 (0, 0)	**0**	30 (**68**, **54**)	0.85	7.5 (28, 47)	**0.04**	0 (0, 0)	**0.01**	0 (0, 0)	**0**	11 (23, 20)	0.73		
S. affinis	9 (19, 17)	0.70	12 (**63**, 15)	**0.99**	11 (33, 17)	**0.98**	0 (0, 0)	0.15	4 (7, 7)	0.70	21 (**100**, 27)	**1**	9 (37, 11)	**1**

Numbers in parentheses represent the percent overlap of species A (column) with species B (row) and vice versa. Numbers in bold represent shared overlap >50%. Second column of numbers represents the likelihood of differences in SEAc size. Numbers in bold represent statistically significant differences in SEAc size between the pair of species examined.

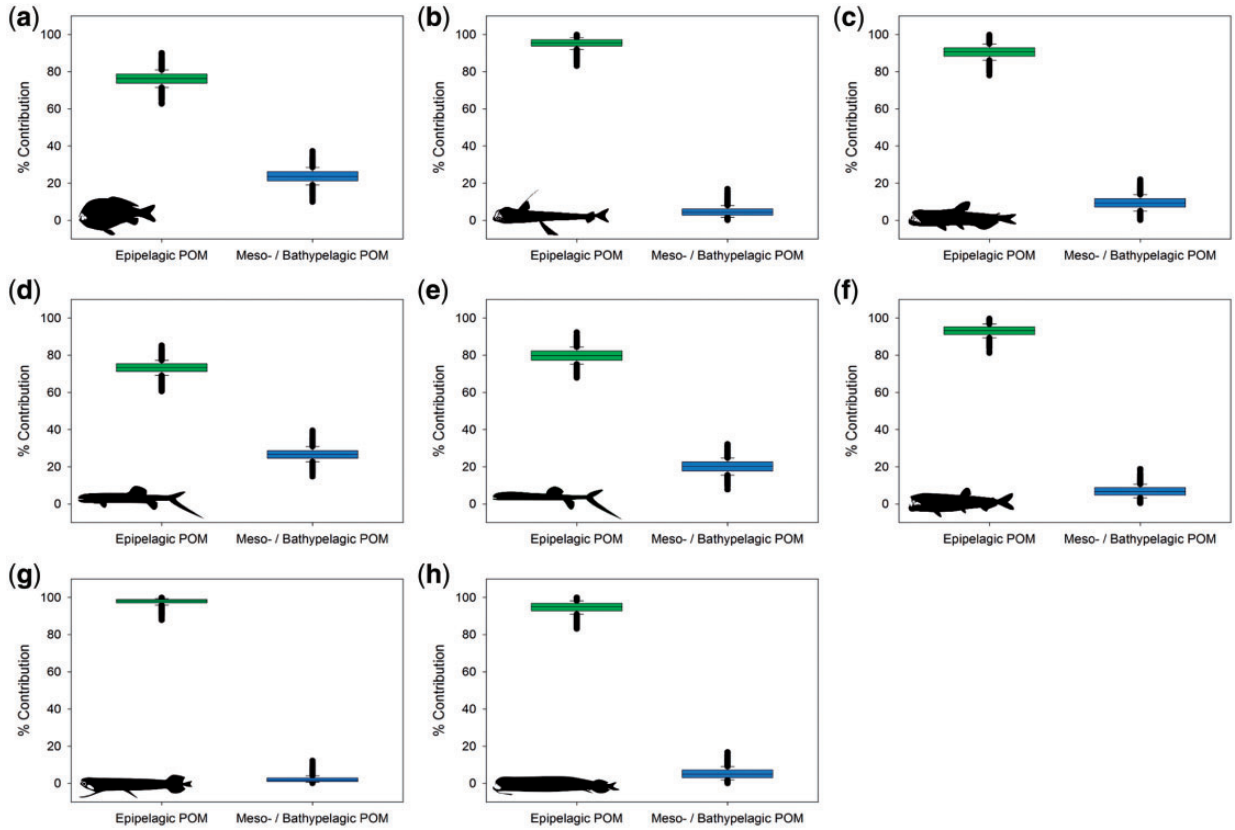

Figure 6. Estimated relative contributions of POM collected from epipelagic and meso- and bathypelagic depths to (a) *A. cornuta*, (b) *C. sloani*, (c) *C. atlantica*, (d) *G. chuni*, (e) *G. indica*, (f) *O. lowii*, (g) *P. guernei*, and (h) *S. affinis*.

between mesoscale cyclonic and anticyclonic oceanographic features (Wissel and Fry, 2005; Dorado *et al.*, 2012, Wells *et al.*, 2017). Baseline differences in POM isotopic signatures between nearshore and offshore environments of the GOM can be caused by phytoplankton in offshore regions relying more heavily on isotopically light nitrogen produced by diazatrophic cyanobacteria (*Trichodesmium* spp.) (Holl *et al.*, 2007; Dorado *et al.*, 2012), while baseline differences between cyclonic and anticyclonic regions are driven by upwelling within cyclonic features supplying ^{15}N enriched N_2 to phytoplankton (Wells *et al.*, 2017). The pattern of POM samples becoming ^{13}C depleted at eastern longitudes and fishes becoming ^{13}C enriched at lower latitudes and western longitudes is consistent with the idea that organisms collected closer to the continental shelf are more likely to be partially supported by terrestrially derived organic matter from the Mississippi River where the effects of *Trichodesmium* spp. and upwelling on baseline $\delta^{15}N$ values are minimal (Dorado *et al.*, 2012).

Ontogenetic shifts in $\delta^{13}C$ and $\delta^{15}N$

Ontogenetic enrichment in ^{15}N was documented in six of the eight species examined. While significant relationships between $\delta^{15}N$ and body size suggest ontogenetic patterns in feeding ecology, observed trends in some cases were driven by a few points, and the nature of size-based relationships with $\delta^{15}N$ could change with the inclusion of different size classes and more samples. Observed enrichment in ^{15}N with body size could be caused by ontogenetic shifts in prey selection, as has been suggested for *A.*

cornuta, C. sloani, and *P. guernei* or by ingestion of larger sized prey (Hopkins *et al.*, 1996; Sutton and Hopkins, 1996b). For species such as *S. affinis* and *C. sloani*, which have been shown to feed on myctophid fishes across their ontogeny, observed positive relationships between $\delta^{15}N$ and body size could be a result of ingestion of larger myctophid fishes, which have been shown to become enriched in ^{15}N with increasing size (Sutton and Hopkins, 1996b; Cherel *et al.*, 2010; McClain-Counts *et al.*, 2017). The negative relationship between body size and $\delta^{15}N$ of *O. lowii* contrasts with published diet data suggesting that *O. lowii* undergoes an ontogenetic diet shift from eating fishes as juveniles to feeding primarily on squid and fish as adults (Rofen, 1966; Hopkins *et al.*, 1996). *Omosudis lowii* are known to have highly distensible stomachs and have been reported to feed on prey much larger than themselves (Rofen, 1966). However, the tendency to feed on large prey appears to occur primarily during juvenile stages, as adults have been found to feed on both large and small prey (Rofen, 1966). Thus, the lack of a relationship between SL and $\delta^{15}N$ of *O. lowii* could be a function of adults and juveniles feeding on similarly sized prey or by switching to prey that occupy lower TPs. The observed relationships between $\delta^{15}N$ and body size are not necessarily the result of ontogenetic shifts in diet and can instead reflect spatial and temporal changes in the isotopic signature of nitrogen sources at the base of the foodweb (Wells *et al.*, 2017). Spatial variation in the isotopic signatures of primary producers has been documented in the GOM, but the increased movements and longer tissue turnover rates of fishes likely diminishes spatial variation by increasing the likelihood of an organism integrating the isotopic signatures of multiple isotopic baselines.

Relative contributions of epi-, meso-, and bathypelagic POM to deep-pelagic fishes

A paradigm of deep-sea ecology is that meso- and bathypelagic organisms feed within foodwebs largely supported by epipelagic POM and that POM suspended at deeper depths contributes little carbon to higher order consumers. Recently, through the use of compound-specific stable isotope analysis (CS-SIA) of amino acids (AAs), that paradigm was challenged by evidence which suggests that zooplankton and micronekton can partly rely on small particle (0.7–53 µm) suspended POM as a carbon source (Hannides *et al.*, 2013; Choy *et al.*, 2015; Gloeckler *et al.*, 2018). Choy *et al.* (2015) estimated the relative contributions of epipelagic and deep-water POM to the production of four fishes (including *A. cornuta*) in the North Pacific and found that two meso- and bathypelagic zooplanktivores received contributions from small-particle, deep-pelagic suspended POM ranging between 39 and 81%, while contributions to the micronektonivore, *A. cornuta*, were far less (0–23%). Gloeckler *et al.* (2018) examined the $\delta^{15}N$ values of source AAs from a micronekton assemblage and found that relative contributions of small, suspended particles to micronekton were greatest in non-migratory species with night-time distributions in the lower mesopelagic and upper bathypelagic. Species with night-time distributions within the epi- and mesopelagic, however, were found to be supported by either surface particles or large, fast-sinking particles (>53 µm) at depth (Hannides *et al.*, 2013; Gloeckler *et al.* 2018).

The results from our mixing-model analyses suggest that the majority of carbon (≥73%) supporting the species examined in this study appears to be derived from epipelagic sources or from fast-sinking particles at depth which carry similar isotopic signatures to particles within the epipelagic (Hannides *et al.*, 2013). These contribution estimates, combined with vertical distribution data which suggest the collective night-time distributions of these predatory fishes span the epi-, meso-, and upper bathypelagic (Sutton and Hopkins, 1996a; Sutton *et al.*, 2010), are in alignment with estimations for micronekton with similar depth distributions made by Choy *et al.* (2015) and Gloeckler *et al.* (2018). It should be noted that the relative contribution of small suspended particles at depth to these species cannot be fully assessed without conducting CSIA-AA and that further investigation into the relative importance of small particles to higher trophic level consumers is warranted (Gloeckler *et al.*, 2018). Additional support for the assertion that these species are largely supported by surface derived carbon is provided by diet studies, which suggest that these species consume migratory prey that feed within food chains supported by surface production (Hopkins *et al.*, 1996; Sutton and Hopkins, 1996b), highlighting the extent to which spatially distinct consumers are connected in the northern GOM.

Supplementary data

Supplementary material is available at the *ICESJMS* online version of the manuscript.

Acknowledgements

We thank Michael Novotny, Nina Pruzinski, and Matthew Woodstock for their help organizing and processing samples. We thank two anonymous reviewers for their comments, which greatly improved this paper. This research was made possible by a grant from the Gulf of Mexico Research Initiative. Data are publicly available through the Gulf of Mexico Research Initiative Information & Data Cooperative (GRIIDC) at https://data.gulfresearchinitiative.org (doi: 10.7266/N7ZS2V04).

References

Angel, M. V. 1997. What is the deep sea? Fish Physiology, 16: 1–41.

Angel, M. V., and Baker, A. 1982. Vertical distribution of the standing crop of plankton and micronekton at three stations in the northeast Atlantic. Biological Oceanography, 2: 1–30.

Caut, S., Angulo, E., and Courchamp, F. 2008. Caution on isotopic model use for analyses of consumer diet. Canadian Journal of Zoology, 86: 438–445.

Cherel, Y., Ducatez, S., Fontaine, C., Richard, P., and Guinet, C. 2008. Stable isotopes reveal the trophic position and mesopelagic fish diet of female southern elephant seals breeding on the Kerguelen Islands. Marine Ecology Progress Series, 370: 239–247.

Cherel, Y., Fontaine, C., Richard, P., and Labatc, J. P. 2010. Isotopic niches and trophic levels of myctophid fishes and their predators in the Southern Ocean. Limnology and Oceanography, 55: 324–332.

Choy, C. A., Davison, P. C., Drazen, J. C., Flynn, A., Gier, E. J., Hoffman, J. C., and McClain-Counts, J. P. 2012. Global trophic position comparison of two dominant mesopelagic fish families (Myctophidae, Stomiidae) using amino acid nitrogen isotopic analyses. PLoS One, 7: e50133.

Choy, C. A., Popp, B. N., Hannides, C. C. S., and Drazen, J. C. 2015. Trophic structure and food resources of epipelagic and mesopelagic fishes in the North Pacific Subtropical Gyre ecosystem inferred from nitrogen isotopic compositions. Limnology and Oceanography, 60: 1156–1171.

Choy, C. A., Portner, E., Iwane, M., and Drazen, J. C. 2013. Diets of five important predatory mesopelagic fishes of the central North Pacific. Marine Ecology Progress Series, 492: 169–184.

Clarke, T. A. 1982. Feeding habits of stomiatoid fishes from Hawaiian waters. Fishery Bulletin, US, 80: 287–304.

Clarke, T. A., and Wagner, P. J. 1976. Vertical distribution and other aspects of the ecology of certain mesopelagic fishes taken near Hawaii. Fishery Bulletin, US, 74: 635–646.

Danovaro, R., Gambi, C., Dell'Anno, A., Corinaldesi, C., Fraschetti, S., Vanreusel, A., and Vincx, M. 2008. Exponential decline of deep-sea ecosystem functioning linked to benthic biodiversity loss. Current Biology, 18: 1–8.

Dorado, S., Rooker, J., Wissel, B., and Quigg, A. 2012. Isotope baseline shifts in pelagic food webs of the Gulf of Mexico. Marine Ecology Progress Series, 464: 37–49.

Drazen, J. C., and Sutton, T. T. 2017. Dining in the deep: the feeding ecology of deep-sea fishes. Annual Review of Marine Science, 9: 337–366.

Fernández-Carrera, A., Rogers, K. L., Weber, S. C., Chanton, J. P., and Montoya, J. P. 2016. Deep water horizon oil and methane carbon entered the food web in the Gulf of Mexico. Limnology and Oceanography, 61: S387–S400.

Gloeckler, K., Choy, C. A., Hannides, C. C. S., Close, H. G., Goetze, E., Popp, B. N., and Drazen, J. C. 2018. Stable isotope analysis of micronekton around Hawaii reveals suspended particles are an important nutritional source in the lower mesopelagic and upper bathypelagic zones. Limnology and Oceanography, 63: 1168–1180.

Gjøsaeter, J., and Kawaguchi, K. 1980. A review of the world resources of mesopelagic fish. FAO Fisheries Technical Report No, 193: 151 pp.

Hannides, C. C. S., Popp, B. N., Choy, C. A., and Drazen, J. C. 2013. Midwater zooplankton and suspended particle dynamics in the North Pacific Subtropical Gyre: a stable isotope perspective. Limnology and Oceanography, 58: 1931–1946.

Hoffman, J. C., and Sutton, T. T. 2010. Lipid correction for carbon stable isotope analysis of deep-sea fishes. Deep-Sea Research Part I: Oceanographic Research Papers, 57: 956–964.

Holl, C. M., Villareal, T. A., Payne, C. D., Clayton, T. D., Hart, C., and Montoya, J. P. 2007. Trichodesmium in the western Gulf of Mexico: 15N2-fixation and natural abundance stable isotope evidence. Limnology and Oceanography, 52: 2249–2259.

Hopkins, T. L., and Gartner, J. V. 1992. Resource-partitioning and predation impact of a low-latitude myctophid community. Marine Biology, 114: 185–197.

Hopkins, T. L., Sutton, T. T., and Lancraft, T. M. 1996. The trophic structure and predation impact of a low latitude midwater fish assemblage. Progress in Oceanography, 38: 205–239.

Hussey, N. E., Macneil, M. A., McMeans, B. C., Olin, J. A., Dudley, S. F. J., Cliff, G., Wintner, S. P. *et al.* 2014. Rescaling the trophic structure of marine food webs. Ecology Letters, 17: 239–250.

Irigoien, X., Klevjer, T. A., Røstad, A., Martinez, U., Boyra, G., Acuña, J. L., Bode, A. *et al.* 2014. Large mesopelagic fishes biomass and trophic efficiency in the open ocean. Nature Communications, 5: 3271.

Jackson, A. L., Inger, R., Parnell, A. C., and Bearhop, S. 2011. Comparing isotopic niche widths among and within communities: SIBER – Stable Isotope Bayesian Ellipses in R. Journal of Animal Ecology, 80: 595–602.

McCann, K. S. 2000. The diversity–stability debate. Nature, 405: 228–233.

McClain-Counts, J. P., Demopoulos, A. W. J., and Ross, S. W. 2017. Trophic structure of mesopelagic fishes in the Gulf of Mexico revealed by gut content and stable isotope analyses. Marine Ecology, 38: e12449–e12423.

McEachran, J. D., and Fechhelm, J. D. 1998. Fishes of the Gulf of Mexico, Volume 1: Myxiniformes to Gasterosteiformes. University of Texas Press, Austin. 1120 pp.

Mengerink, K. J., Dover, C. L., Van Ardron, J., Baker, M., Escobar-briones, E., Gjerde, K., Koslow, J. A. *et al.* 2014. A call for deep-ocean stewardship. Science, 344: 696–698.

Moore, J. A., Vecchione, M., Collette, B. B., Gibbons, R., Hartel, K. E., Galbraith, J. K., Turnipseed, M. *et al.* 2003. Biodiversity of Bear Seamount, New England Seamount chain: results of exploratory trawling. Journal of Northwest Atlantic Fishery Science, 31: 363–372.

Morato, T., Watson, R., Pitcher, T. J., and Pauly, D. 2006. Fishing down the deep. Fish and Fisheries, 7: 24–34.

Moteki, M., Arai, M., Tsuchiya, K., and Okamoto, H. 2001. Composition of piscine prey in the diet of large pelagic fish in the eastern tropical Pacific Ocean. Fisheries Science, 67: 1063–1074.

Pakhomov, E. A., Perissinotto, R., and McQuaid, C. D. 1996. Prey composition and daily rations of myctophid fishes in the Southern Ocean. Marine Ecology Progress Series, 134: 1–14.

Pauly, D., Trites, A. W., Capuli, E., and Christensen, V. 1998. Diet composition and trophic levels of marine mammals. ICES Journal of Marine Science, 55: 467–481.

Peterson, B. J., and Fry, B. 1987. Stable isotopes in ecosystem studies. Annual Review of Ecology and Systematics, 18: 293–320.

Polis, G. A., and Strong, D. R. 1996. Food web complexity and community dynamics. The American Naturalist, 147: 813–846.

Porteiro, F. M., and Sutton, T. T. 2007. Midwater fish assemblages and seamounts. *In* Seamounts: Ecology, Conservation and Management, pp. 101–116. Ed. by T. J. Pitcher, T. Morato, P. J. B. Hart, M. R. Clark, N. Haggan, and R. S. Santos. Blackwell, Fish and Aquatic Resources Series, Oxford. 552 pp.

Post, D. M. 2002. Using stable isotopes to estimate trophic position: models, methods, and assumptions. Ecology, 83: 703–718.

Post, D. M., Layman, C. A., Arrington, D. A., Takimoto, G., Quattrochi, J., and Montaña, C. G. 2007. Getting to the fat of the matter: models, methods and assumptions for dealing with lipids in stable isotope analyses. Oecologia, 152: 179–189.

R Development Core Team. 2016. R: a language and environment for statistical computing. R Foundation for Statistical Computing, Vienna. www.R-project.org.

Raclot, T., Groscolas, R., and Cherel, Y. 1998. Fatty acid evidence for the importance of myctophid fishes in the diet of king penguins, *Aptenodytes patagonicus*. Marine Biology, 132: 523–533.

Ramirez-Llodra, E., Tyler, P. A., Baker, M. C., Bergstad, O. A., Clark, M. R., Escobar, E., Levin, L. A. *et al.* 2011. Man and the last great wilderness: human impact on the deep sea. PLoS One, doi.org/10.1371/journal.pone.0022588

Robison, B. H. 2004. Deep pelagic biology. Journal of Experimental Marine Biology and Ecology, 300: 253–272.

Robison, B. H. 2009. Conservation of deep pelagic biodiversity. Conservation. Biology, 23: 847–858.

Rofen, R. R., 1966. Family Omosudidae. *In* Fishes of the Western North Atlantic. Memoir No. 1. Part 5, pp. 464–481. Ed. by H. G. Bigelow, C. M. Breder, Y. H. Olsen, D. M. Cohen, W. C. Schroeder, G. H. Mead, L. P. Schultz *et al.* Sears Foundation for Marine Research, Yale University, New Haven, CT.

Stock, B. C., Semmens, B. X. 2015. MixSIAR GUI user manual, version 1.0. http://conserver.iugo-cafe.org/user/brice.semmens.

Sutton, T. T. 2013. Vertical ecology of the pelagic ocean: classical patterns and new perspectives. Journal of Fish Biology, 83: 1508–1527.

Sutton, T. T., and Hopkins, T. L. 1996a. Species composition, abundance, and vertical distribution of the stomiid (Pisces: Stomiiformes) assemblage in the Gulf of Mexico. Bulletin of Marine Science, 59: 530–542.

Sutton, T. T., and Hopkins, T. L. 1996b. Trophic ecology of the stomiid (Pisces: Stomiidae) fish assemblage of the eastern Gulf of Mexico: strategies, selectivity and impact of a top mesopelagic predator group. Marine Biology, 127: 179–192.

Sutton, T. T., Porteiro, F. M., Heino, M., Byrkjedal, I., Langhelle, G., Anderson, C. I. H., Horne, J. *et al.* 2008. Vertical structure, biomass and topographic association of deep-pelagic fishes in relation to a mid-ocean ridge system. Deep Sea Research Part II: Topical Studies in Oceanography, 55: 161–184.

Sutton, T. T., Wiebe, P. H., Madin, L., and Bucklin, A. 2010. Diversity and community structure of pelagic fishes to 5000 m depth in the Sargasso Sea. Deep-Sea Research Part II: Topical Studies in Oceanography, 57: 2220–2233.

Sweeting, C. J., Barry, J., Barnes, C., Polunin, N. V. C., and Jennings, S. 2007. Effects of body size and environment on diet-tissue15N fractionation in fishes. Journal of Experimental Marine Biology and Ecology, 340: 1–10.

Sweeting, C. J., Barry, J. T., Polunin, N. V. C., and Jennings, S. 2007. Effects of body size and environment on diet-tissue13C fractionation in fishes. Journal of Experimental Marine Biology and Ecology, 352: 165–176.

Thurber, A. R., Sweetman, A. K., Narayanaswamy, B.E., Jones, D. O. B., Ingels, J., and Hansman, R. L. 2014. Ecosystem function and services provided by the deep sea. Biogeosciences, 11: 3941–3963.

Trueman, C. N., Johnston, G., O'Hea, B., and MacKenzie, K. M. 2014. Trophic interactions of fish communities at midwater depths enhance long-term carbon storage and benthic production on continental slopes. Proceedings of the Royal Society B: Biological Sciences, 281: 20140669–20140669.

Valls, M., Olivar, M. P., Fernández de Puelles, M. L., Molí, B., Bernal, A., and Sweeting, C. J. 2014. Trophic structure of mesopelagic fishes in the western Mediterranean based on stable isotopes of carbon and nitrogen. Journal of Marine Systems, 138: 160–170.

Webb, T. J., Vanden Berghe, E., and O'Dor, R. 2010. Biodiversity's big wet secret: the global distribution of marine biological records reveals chronic under-exploration of the deep pelagic ocean. PLoS One, 5: e10223–e10226.

Wells, R. J. D., Rooker, J. R., Quigg, A., and Wissel, B. 2017. Influence of mesoscale oceanographic features on pelagic food webs in the Gulf of Mexico. Marine Biology, 164: 1–11.

Wilson, R. W., Millero, F. J., Taylor, J. R., Walsh, P. J., Christensen, V., Jennings, S., and Grosell, M. 2009. Contribution of fish to the marine inorganic carbon cycle. Science, 323: 359–362.

Wissel, B., and Fry, B. 2005. Tracing Mississippi River influences in estuarine food webs of coastal Louisiana. Oecologia, 144: 659–672.

Handling editor: Emory Anderson